Excitonics: A universal set of binary gates for molecular exciton processing and signaling

Nicolas P. D. Sawaya, Dmitrij Rappoport, Daniel P. Tabor, and Alán Aspuru-Guzik*
Department of Chemistry and Chemical Biology, Harvard University,
12 Oxford St, Cambridge, Massachusetts 02138, USA
(Dated: August 14, 2017)

The ability to regulate energy transfer pathways through materials is an important goal of nanotechnology, as a greater degree of control is crucial for developing sensing, solar energy, and bioimaging applications. Such control necessitates a toolbox of actuation methods that can direct energy transfer based on user input. Here we propose a novel molecular exciton gate, analogous to a traditional transistor, for controlling exciton migration in chromophoric systems. The gate may be activated with an input of light or an input flow of excitons. Unlike previous gates and switches that control exciton transfer, our proposal does not require isomerization or molecular rearrangement, instead relying on excitation migration via the second singlet (S2) state of the gate molecule–hence the system is named an "S2 exciton gate." After presenting a set of system properties required for proper function of the S2 exciton gate, we show how one would overcome the two possible challenges: short-lived excited states and suppression of false positives. Precision and error rates are studied computationally in a model system with respect to excited-state decay rates and variations in molecular orientation. Finally, we demonstrate that the S2 exciton gate gate can be used to produce binary logical AND, OR, and NOT operations, providing a universal excitonic computation platform with a range of potential applications, including e.g. in signal processing for microscopy.

I. INTRODUCTION

Developing ways to reliably direct energy transfer on the nanoscale would allow for the development of new nanoscopic devices for bioimaging, photocatalysis, and sensing. Here we propose a new type of elementary component of such devices, an exciton gate, that uses multiply-excited states to direct and control the flow of excitons in organic molecules.

The concept of a *gate* is essential in many areas of engineering and science. Ubiquitous gate-like devices include field effect transistors in computing, relays used in larger electronics, and valves for controlling liquid flow in civil engineering. The ability to regulate flow allows one to direct the movement of energy and mass, or allows one to build complex logic devices like the modern computer. The concept is implementable beyond electrical current and liquids. For instance, a number of exotic media have been used to implement logic gates, notably using DNA structures [1] and optical materials [2]. Many other nanoscopic transistor-like devices have been theoretically proposed or experimentally implemented, including single-molecule electrical transistors [3], light-activated solid-state semiconductor excitonic gates [4, 5], and so-called electrothermal transistors [6].

Several schemes have previously been developed for controlling energy transfer in interacting chromophoric systems [7], by developing switches that can be toggled between an on state and an off state. Generally, previous methods exploit isomerization reactions [8, 9]. The molecule's resulting conformation has a modified energy gap, transition dipole orientation, and/or position. Because structural changes in the chromophores affect the detuning and dipole–dipole coupling between the transitions of two interacting chromophores, the energy transfer speed and efficiency are changed. Isomerizations in light-interacting molecules can be achieved by various control inputs, including laser light [7], strain [10], or pH change [11].

Structural isomerizations involve substantial rearrangement of the nuclear frame and thus generally occur on a timescale of picoseconds to hundreds of picoseconds [12]. A motivation for this work is to invent faster gate actuation methods that avoid large-amplitude nuclear displacement, by using both the first and second excited states of a relatively rigid molecule. Our strategy may hold advantages over isomerization-based gating techniques for the following reasons:

1. Our scheme may potentially yield faster gate switching times,

2. Chemical systems which do not change shape in uncontrollable ways may be easier to use in applications,

3. Commonly used isomerization reactions require high-energy ultraviolet light, which may be damaging to the exciton circuit or to nearby chemical species,

4. The isomerization route allows for discrete binary logic but not for a continuous transistor-like behavior of "gain," while our strategy may allow for both, and

* aspuru@chemistry.harvard.edu; Additional affiliation: Senior Fellow, Canadian Institute for Advanced Research, Bioinspired Solar Energy Program, Toronto, ON M5G 1Z8, Canada

5. Developing more general strategies for gate designs will increase the likelihood that designs can be found for arbitrary applications.

In this theoretical study, we introduce an "exciton gate" in which an exciton behaves as the fluid or current, and the control input is provided by external light or by the flow of auxiliary excitons. The gate itself is a molecule considered to be "off" in its ground singlet state (S0) and "on" in its first excited singlet state (S1). As described in Section II, when the gate is turn on, excitation energy flows through the second singlet state (S2), while no current flows when the gate is off.

Because this design allows for binary logic and exciton signal processing, we anticipate that one potential application of this "S2 exciton gate" will be as a building block in a new class of biomarkers. For instance, one would be able to use external light to probe the truth of a logical clause like "a AND NOT b OR (c AND NOT d)," where binary variables a through d denote the presence of a specific macromolecule or a particular molecular conformation. Arithmetic, including addition and subtraction, can also be carried out with these same logical operations.

The development of excitonic circuits may allow for multiplexing and conditional (e.g. logic-based) signals that were not possible before. More complex circuits may allow a small number of dyes to have a large number of input-dependent outputs. For example, if one can control four independent exciton gates in a circuit, in principle this provides up to $2^4 = 16$ unique output signals, which may be one way to escape the line width limitations [13] arising from using one dye per output variable, while using even fewer dyes. Other more exotic applications may include complex directed photocatalyis, phototherapeutics, chemical sensing, or new experimental methods for studying the behavior of excitonic systems such as photosynthetic complexes.

A successful experimental implementation of an S2 exciton gate scheme involves two major challenges, which we demonstrate how to overcome in this theoretical study. The gate's operation and the two main implementation obstacles are given in Section II and viable molecular candidates are discussed in Section III. Multiple designs for binary logic operations are given in Section IV. Errors due to imprecise molecular orientations are discussed in Section V. Model simulations are then presented in Section VI before concluding remarks are given in Section VII.

II. S2 EXCITON GATE

Consider three molecules, denoted C, G, and E (labels in this paper are chosen in analogy to the bipolar junction transistor's (BJT) electrodes, in which C and E refer to collector and base). G will be called the gate molecule, while C and E are the input and output molecules, respectively.

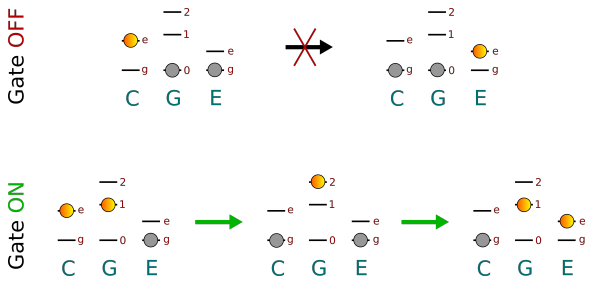

FIG. 1: Schematic of the S2 exciton gate concept. C, G, and E denote organic molecules. States g and e are electronic singlet ground and excited states, respectively. States 0, 1, and 2 are the ground, first excited singlet, and second excited singlet states of molecule G. The exciton gate is OFF (top) when G is in its ground state $G0$. In this case, the energy levels forbid an exciton on C from migrating through G. Conversely, the exciton gate is ON (bottom) when G is in state $G1$. Because the energy gap $\epsilon[G2] - \epsilon[G1]$ is less than or on resonance with $\epsilon[Ce] - \epsilon[Cg]$, energy can now flow through G via the $G2$ state. There are two main challenges that are the likely reasons for this scheme not having been hitherto proposed or implemented: (a) one must suppress multiple undesired transfer processes, e.g. from $G1$ to Ce and (b) one must use molecules with relatively long-lived second excited singlet states. The present theoretical paper demonstrates how both challenges can be overcome.

The molecular electronic states are denoted as follows. In molecule C, Cg is the ground state and Ce is the first excited singlet state. In G, the $G0$ is the ground state, $G1$ is the first excited singlet state, and $G2$ is the second excited singlet state. To simplify notation, $G0$, $G1$, and $G2$ are also to be referred to as 0, 1, and 2, respectively. Eg and Ee are the ground and first excited singlet states of molecule E. $\epsilon[A]$ denotes the energy of state A, and $\mu[A_x^y]$, with norm $\hat{\mu}[A_x^y]$, denotes the transition dipole between molecule A's two electronic states x and y. $V[A_x^y, B_w^z]$ denotes the dipole–dipole interaction between molecule A's $x \to y$ transition and molecule B's $w \to z$ transition. Hence V determines the rate at which an excitation transfer between two electronic states.

These molecules are chosen such that $\epsilon[Ce] - \epsilon[Cg]$ is less than $\epsilon[G1] - \epsilon[G0]$ (see Figure 1), and such that $\epsilon[Ce] - \epsilon[Cg]$ is greater than or on resonance with $\epsilon[G2] - \epsilon[G1]$. Consider the system starting in state $(Ce, G0, Eg)$. In this OFF state, energy alignment prevents the exciton from moving through molecule G. However, if the initial state is $(Ce, G1, Eg)$, the system is in the ON state, and the exciton may migrate through the $G2$ state and onto the Ee state.

Certain design advantages are immediately apparent. The first is that, for most organic molecules, the S1–S2 gap tends to be smaller than the S0–S1 gap. The second advantage is the enormous molecular space from which one can choose dyes with appropriate properties,

including energy gaps, transition dipole strengths, and exciton decay times. Third, it is not necessary to consider complex quantum effects and delocalization. In other words, the scheme can function in the incoherent Förster regime.

Though our proposed gating concept is conceptually very simple, we think that the reason it has not been previously proposed is that two significant roadblocks to a viable design are clear from the outset. The first is that the vast majority of organic molecules have short-lived S2 states (0.1 to 10 picoseconds [14]), as internal conversion normally causes fast decay to the first excited (S1) state. This behavior is related to the well-known rule of Kasha [15], which states that fluorescence tends to be observed only from the S1 state. Undesired decay can also occur via intersystem crossing to a triplet state. Fortunately there are known dye classes for which longer-lived S2 states are possible, as discussed in Section III. Additionally, faulty but possibly useful gates may realizable even using dyes with quite average S2 lifetimes, as shown via simulations in Section VI.

The second roadblock is the problem of suppressing undesired additional exciton transfer pathways. Most important to consider is an exciton moving from the $G1$ to the Ee state (Figure 2). Since an excitation can end up in Ce without Ce ever having been populated, the process leads to a certain probability of false positives. Here we describe briefly how this undesired transfer can be suppressed, before elaborating further in Section V.

In the incoherent Förster regime, transfer rates are parameterized by two quantities: the overlap integral between the donor emission and the acceptor absorption spectra, and the relative orientation of the two transition dipoles [16]. (The overlap integral of course depends implicitly on the energy gaps and transition dipoles strengths of the two dyes.) The orientation factor κ is defined as

$$\kappa = \hat{\mu}_D \cdot \hat{\mu}_A - 3(\hat{\mu}_D \cdot \hat{r})(\hat{\mu}_A \cdot \hat{r}) \quad (1)$$

where $\hat{\mu}_D$ and $\hat{\mu}_A$ are unit vectors of the donor and acceptor transition dipole moments, respectively, and $\hat{r}$ is the unit vector for the displacement between the donor and acceptor. In the dipole-dipole approximation, when $\kappa = 0$ there is no energy transfer. The range of κ is from -2 to +1. Because κ=0 is allowed, one can eliminate transfer between two exciton states, assuming one has control over dipole orientations. In a planar orientation, $\kappa = 0$ occurs at the so-called magic angle of approximately 54.7°. Until recently, precise control of the relative orientations would be impossible. Fortunately, recent developments in nanoscale design provide promising methods for implementing orientational constraints (see Section V).

In order to design an ideal exciton gate, several energy gaps must be aligned and multiple transfer processes must be suppressed. In summary, the following conditions must be met:

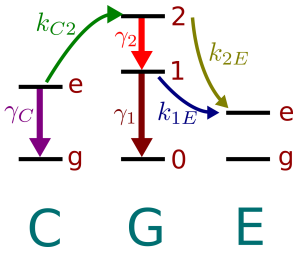

FIG. 2: Schematic of competing rates in the exciton gate, where k's denote transfer rate and γ's denote decay rates. An optimal gate design yields k_{1E} and all γ as small as possible.

1. $\epsilon[Ce] - \epsilon[Cg] < \epsilon[G1] - \epsilon[G0]$. C's S0-S1 energy gap must be smaller than G's S0-S1 gap.
2. $\epsilon[Ce] - \epsilon[Cg] \geq \epsilon[G2] - \epsilon[G1]$. C's S0-S1 energy gap must be greater than or on resonance with G's S1-S2 gap.
3. $\epsilon[G2] - \epsilon[G1] \geq \epsilon[Ee] - \epsilon[Eg]$. G's S1-S2 energy gap must be greater than or on resonance with E's S0-S1 gap.
4. $V[C_e^g, G_0^1] = 0$. Suppress transfer from $G1$ to Ce.
5. $V[G_0^1, E_g^e] = 0$. Suppress transfer from $G1$ to Ee.
6. $V[C_g^e, G_1^2] \neq 0$. Appreciable transfer needed between state $(Ce, G1)$ and state $(Cg, G2)$.
7. $V[G_1^2, E_g^e] \neq 0$. Appreciable transfer needed between state $(G2, E0)$ and state $(G1, Ee)$.

Note that these conditions lead to the implicit (redundant) condition that $\hat{\mu}[G_0^1] \neq \hat{\mu}[G_1^2]$, i.e. the transition dipole for $G0 \rightarrow G1$ must point in a different direction than $G1 \rightarrow G2$.

III. CHOOSING GATE DYES

There are tens of thousands of dyes from which to choose molecules C and E, absorbing and emitting at virtually any visible frequency. These dyes are commercially available and cataloged, and the energy levels simply need to be lined up according to the design constraints.

It is more difficult to choose an appropriate gate molecule, G. It is important to reiterate that, though the first experimental implementations of an S2 exciton gate will likely produce imperfect and lossy gates, even a very lossy exciton gate may be useful in applications (see Section VI). Still, candidates with S2 states that are longer-lived than 10 ps are the best candidates for G molecules, but such molecule likely comprise a very small fraction of the full molecular space. However, it has been estimated that the number of small molecules that can be made from 30 atoms may exceed 10^{60} [17], many of which

may be as good or better than the candidates discussed below. It appears that small symmetric molecules are the most promising option, as there are already known classes of such molecules that violate Kasha's rule.

There are in fact a number of promising known molecule classes, which we summarize here. This list is meant as a guide for choosing appropriate S2 molecules in the future, including via high-throughput screening [18]. Note that one investigative difficulty is that there are absorption (i.e. S1-related information) profiles for many dyes, but the literature does not contain nearly as many molecules whose S2 states have been studied (e.g. via transient absorption spectroscopy).

Azulene derivatives. Azulene was one of the first molecules to exhibit substantial fluorescence from the S2 $\rightarrow$ S0 transition [19]. Many derivatives that show the same effect have since been synthesized [20–23]. This S2 fluorescence violates Kasha's rule, which states that an S2 state decays to S1 very quickly, such that fluorescence is seen only from the S1 state. Azulene's S2 lifetime is approximately 1 nanosecond, its S1 lifetime is relatively short at approximately 1 picosecond, and theoretical calculations have shown that both S0 $\rightarrow$ S1 and S1 $\rightarrow$ S2 transitions are appreciable and are of similar orders of magnitude [24]. However, synthesizing additional azulene derivatives with new functional groups may lead to a dye in which both S1 and S2 states have lifetime that exceed 10 or even 100 ps, while providing a method for tuning the energy gaps. But even a short-lived S1 state such as azulene's would be very amenable to the four-molecule gate construction given in Section IV, because the S1 state is continually being populated by a steady-state stream of excitons.

Polyenes with C2h symmetry may be viable candidates, as some such molecules have been shown to violate Kasha's rule [25–27]. However, the character and ordering of the excited states is strongly structure- and substitution-dependent, and there is still some controversy in the interpretation of the experimental and computational results for some prototypical polyenes. At the same time, the structure dependence may be a useful source of variety in generating viable candidates.

Molecules with charge-transfer (CT) excited states may be promising as well, since their metastable excited states are often longer-lived than non-CT excited states. However, transition dipole moments for CT states are usually smaller than non-CT transitions. Because long-range charge transfer excitations are usually accompanied by a significant rearrangement of the nuclear frame [12, 14], the transition dipoles of excitation and de-excitation may not be equal. This may require a change in the orientational constraints for the gate design, since the original constrains assumed an equal excitation and de-excitation transition dipole.

Coherent heterodimer. Assuming one had precise geometric control, an encouraging route is to create a single strongly interacting dimer to behave as a gate molecule. This allows one to tune the positions of the excited states directly, by choosing the relative distance, the orientations, and the dyes themselves. One can show that such a scheme must use a heterodimer, because in the case of a homodimer, the $\mu[G_0^1]$ and $\mu[G_1^2]$ transition dipoles are oriented in the same direction [28], which would violate the constraints. Further details for a dimer design of G are provided in Appendix B.

Screening. Keeping the above classes of molecules in mind, it is possible to screen a large library of candidates, as has been done for a variety of other applications, for example in developing organic light emitting diodes [18]. We have performed a screening of analysis of one class of compounds, as described in Appendix D. As with other screening protocols, here molecules are filtered out based on successive criteria, with the more computationally demanding calculations reserved for smaller pools of molecules that satisfy the computationally cheaper to calculate criteria. A scoring function would rates molecules based on (a) appreciable S0 $\rightarrow$ S1 and S1 $\rightarrow$ S2 transitions, (b) S0 $\rightarrow$ S1 and S1 $\rightarrow$ S2 transition dipoles having nonidentical orientations relative to each other, (c) both energy gaps being in the visible range (as background infrared noise would interfere with the gate's function, and ultraviolet light tends to damage organic molecules), (d) no easily accessible triplet states in the vicinity of the relevant energies in order to avoid intersystem crossing, and (e) S1 and S2 states as long-lived as possible, based in part on the accessibility of nearby conical intersections [29–31].

In an initial screening procedure for this study, we developed a first-pass scoring function that rates molecules based on criteria (a) through (d). For a highly restricted dataset of just 180 azulene-like molecules, we found 40 reasonable candidates for G molecules. Further details are provided in Appendix D.

Once a library of gate molecules is found, the appropriate C and E partners for each gate molecule can be trivially found from large known dye libraries, based on the required band gaps for the C and E molecules.

IV. UNIVERSAL LOGIC GATE SETS

In this section we provide designs for organic exciton logic gates, in analogy to traditional solid-state transistors. Consider the NPN bipolar junction transistor (BJT), though the analogy is appropriate for other transistors including field-effect transistors. The transistor itself is like the S2 exciton gate (G molecule). The collector (C) terminal can be compared to our C molecule, and the emitter (E) terminal to our E molecule. In the BJT, the base (B) terminal is the input that "switches" the gate on, allowing current to flow.

One may activate the gate molecule by shining light with frequency on resonance with G's S0-S1 gap. We call this the three-molecule construction. In this case, it can be said that the light source behaves as the base (B) terminal. One drawback of using light to activate

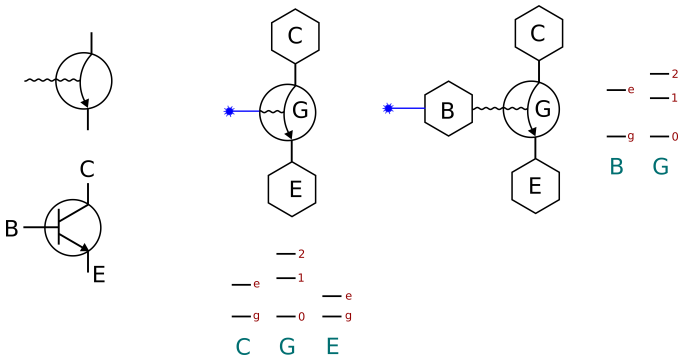

FIG. 3: Bottom Left: Symbol for a bipolar junction transistor, with emitter (E), base (B) and collector (C) electrodes. Top left: Symbol for an S2 exciton gate. Center: Three-molecule construction, with incident light (denoted by a blue line and asterisk) controlling the gate molecule G. Right: Four-molecule construction, with exciton flow from molecule B providing control of the gate. B may be pumped by a light source, analogously to the pumping that is performed in a three-level laser to produce high population in the first excited state.

the gate is that it is not possible (even theoretically) to achieve a steady-state population greater than 50% in the excited state $G1$, by directly pumping the state with light [32].

To overcome this low-population limitation and reach arbitrarily high populations of ON states, the base terminal may instead be mimicked by a fourth molecule, molecule B, that feeds excitons into the S2 gate. We

With these three operations, one can implement universal binary logic, which in principle can in turn be used for computations ranging from solving boolean satisfiability problems to performing arithmetic. (Universal classical computation is possible with only AND and NOT, or with only OR and NOT.)

We first design binary operations that are the direct analogues of the BJT implementations AND, OR, and NOT operations. We call these "Type A" constructions. Next we show alternative constructions, which are more tailored to the S2 exciton gate, which we call "Type B" constructions. The Type B constructions use fewer molecules, and hence require fewer geometric constraints.

In early experimental implementations, all of these operations are likely to have imperfect fidelities, due to incorrect orientations and nonzero decay rates. However, even imperfect gates may find applications, as demonstrated in Section VI.

The NOT implementations merit additional discussion. Type A is entirely analogous to a traditional transistor's NOT scheme, but in the excitonic case it would be leaky even if the excited-state lifetimes were infinite and the orientations were perfect. This is because there is always a non-zero probability that the exciton from the top-left molecule migrates to the OUT molecule, even when G is turned on. This migration from C to OUT can be suppressed by making the $C-G2$ interaction much stronger than the C–OUT interaction, but even in theory the operation cannot be perfect. Both AND types, both OR types, and the Type B NOT implementation, on the other hand, would in principle have perfect fidelity under the ideal conditions of infinite lifetimes and perfect orientations.

The Type B NOT operation does not use the same exciton gate as before. This operation is itself an exciton gate similar to our initial 3-molecule $C-G-E$ exciton gate. Unlike the original exciton gate, the Type B NOT gate transfers energy via the S1 state, and the S2 state is used to suppress transfer. The excitation is allowed to transfer from C to E via the $G1$ state–this is just standard FRET (Förster resonant energy transfer) transfer via the S1 states of each of the three molecules. Hence when G begins in the $G0$ state, the input is binary-0, and the output is 1 (= NOT 0), denoted by population in the Ee state. On the other hand, the state $G2$ corresponds to an input of 1, which suppresses transfer and produces an output of 0 (= NOT 1), e.g. E remains in its ground state. Quite different from the S2 exciton gate, the Type B NOT operation requires the following constraints:

(a) $\epsilon[Ce]-\epsilon[Cg] \geq \epsilon[G1]-\epsilon[G0]$. C's S0–S1 gap is greater

call this the four-molecule construction. The exciton migrates from the Be state (B's S1 state) to the $G1$ state. This fourth molecule may itself be activated by an external light source, or by an exciton flowing from yet another set of chromophores (Figure 3). In other words, in the four-molecule construction the B molecule would be "pumped," in the same way that a three-level laser is pumped to provide population inversion.

This fourth molecule necessitates additional constraints. In addition to those outlined above, these constraints are necessary:

8. $\epsilon[Be]-\epsilon[Bg] \geq \epsilon[G1]-\epsilon[G0]$. B's S0–S1 energy gap must be greater than or on resonance with G's S0–S1 gap. .

9. $V[B^e_g, G^2_1] = 0$. Suppress transfer from Be to $G2$.

10. $V[B^e_g, C^e_g] = 0$. Suppress transfer from Be to Ce.

11. $V[B^e_g, E^e_g] = 0$. Suppress transfer from Be to Ee.

12. $V[B^e_g, G^1_0] \neq 0$. Appreciable transfer needed between states Be and $G1$.

The S2 exciton gate can be used to create a set of universal binary logic operations. Figure 4 shows how one would create the AND, OR, and NOT gates, from which all other binary operators can be made. To connect the gates, the output exciton from one S2 exciton gate may be used as input to the next exciton gate. In other words, one gate molecule can serve as either the C or B molecule of the next gate.

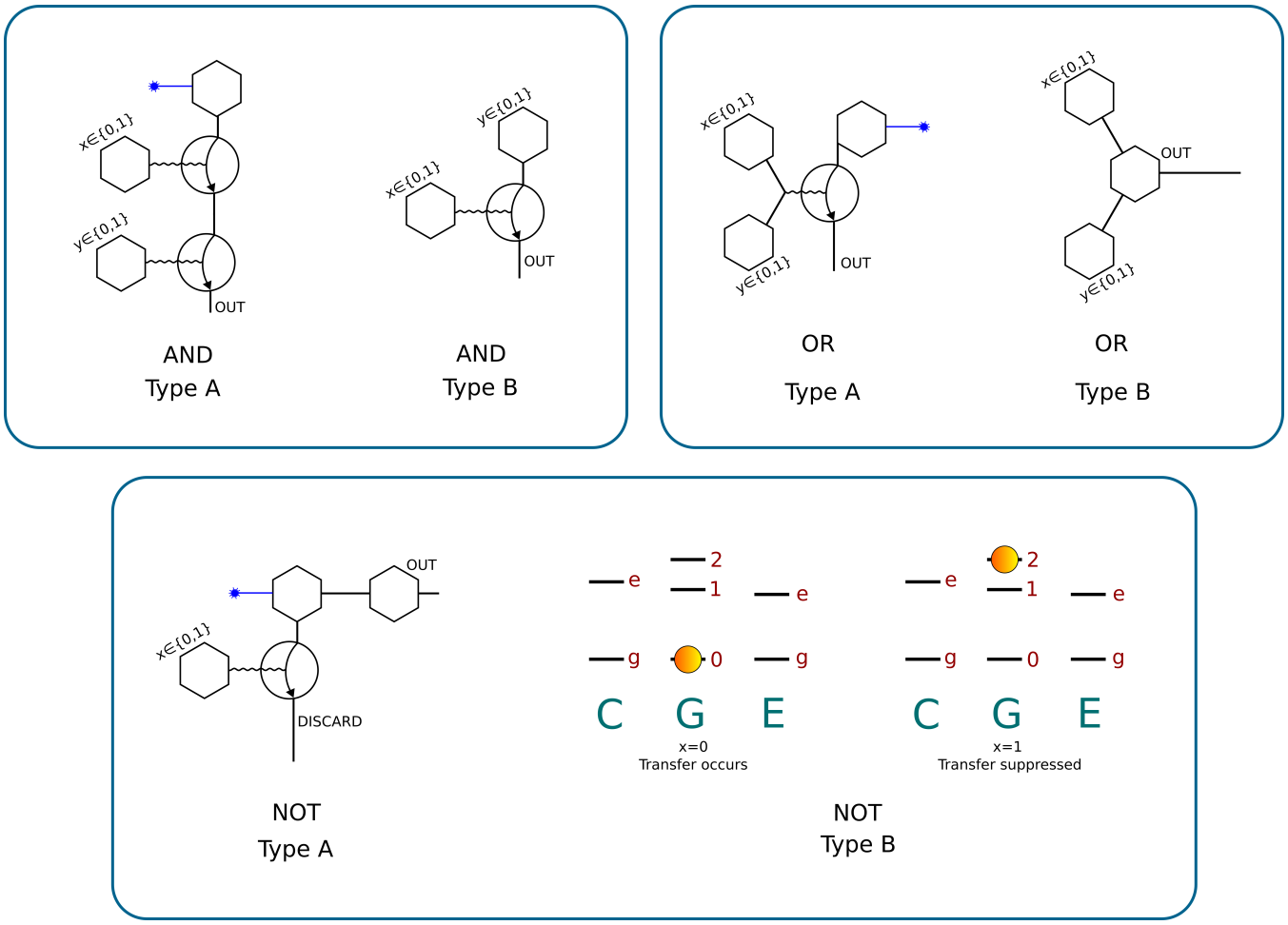

FIG. 4: Schematics of the exciton binary logic gates AND, OR, and NOT. The blue line and asterisk denote input of light. The OUT terminal may connect to a fluorescing molecule, or to an additional binary operation as part of a larger circuit. Universal computation is achievable with AND and NOT gates alone, or with OR and NOT gates alone. For each binary operation, Type A mimics one particular construction (of many) of a traditional electronic transistor-based operation, while Type B is a schematic that is unique to excitonic computation and requires fewer resources.

than or on resonance with G's S0–S1 gap.

(b) $\epsilon[G1]-\epsilon[G0] \geq \epsilon[Ee]-\epsilon[Eg]$. G's S0–S1 gap is greater than or on resonance with E's S0–S1 gap.

(c) $V[C_g^e, G_0^1] > 0$. Appreciable transfer needed between states Ce and $G1$.

(d) $V[G_0^1, C_g^e] > 0$. Appreciable transfer needed from $G1$ to Ce.

(e) $V[G_0^2, C_g^e] = 0$. Transfer is suppressed from $G2$ to Ce.

(f) $V[G_0^2, E_g^e] = 0$. Transfer is suppressed from $G2$ to Ee.

(g) $G2$ decays nearly exclusively directly to $G0$. If $G2$ instead decayed via $G1$, then state $G1$ would transfer to Ee, leading to a false positive. Azulene and its derivatives are again promising candidates, as $G2$ decays primarily to the ground state.

Constraints (e) and (f) can again be satisfied either by magic orientations or by choosing molecules that yield zero absorption-emission overlap between the two transitions. In the limit of ideal conditions, this makes it possible to implement a NOT gate of perfect fidelity, unlike in the case of the Type A NOT operation. As before, the G molecule of the Type B NOT operation can be activated by pumping an auxiliary B molecule.

V. ERRORS AND ORIENTATIONAL CONSTRAINTS

Consider constraints 4 and 5 ($V[C_e^g, G_0^1]= 0$ and $V[G_0^1, E_g^e]= 0$). Each of these transition pairs must be

either detuned such that the emission-absorption overlap is nearly zero, or the value of κ must be near zero. (Note also that the implicit condition $\hat{\mu}[01] \neq \hat{\mu}[12]$ need not be met if both transition pairs are substantially detuned.) When two dipoles are planar, the angle at which $\kappa = 0$ is called the magic angle. If neither of these two dipole pairs are detuned, then κ ought to be near zero for both pairs. This is achievable even in a planar configuration.

Until recent years, it would be virtually impossible to control molecular orientation. However, advancements in synthetic methods to control the nanoscale have placed precise nanoscopic control within reach. DNA nanotechnology, also called DNA origami, is likely the most viable option. Not only has DNA been used to produce a variety of arbitrary shapes and patterns [33], there are also a variety of attachment sites available [34], which provides many options for placing a molecule in a precise orientation. It may be possible to use other tunable nanoscopic methods as well, such as metal-organic frameworks [35] and configurations similar to donor-bridge-acceptor molecules [36].

Note that, because tuning κ for various pairs depends on orientations but not distances, the number of degrees of freedom in the problem is $N_{DOF} = 4m-5-N_C$, where $m > 1$ is the number of molecules and N_C is the number of constraints (i.e. the number of pairs for which $\kappa = 0$). Every new molecule yields a new distance unit vector $\hat{r}$ and transition dipole vector $\hat{\mu}$, each of which introduces new azimuthal and polar angles. Hence four additional orientational (i.e. angular) DOFs are introduced per new molecule. $N_{DOF} = 7$ for the three-molecule construction, since the number of constraints $N_C = 2$.

It is trivial to meet conditions 4 and 5 simultaneously, by assuming a planar arrangement for all transition dipoles. In the general non-planar case, there is a multidimensional manifold (because $N_{DOF} = 7$) over which both conditions are met, which we call the magic manifold. This continuum of many allowable orientations provides multiple routes for synthesizing a viable S2 gate.

If the fourth "base" molecule B is included, then conditions 10, 11, and 9 must be met as well. This yields $N_{DOF} = 11$ from $N_C = 5$, which again provides a multidimensional magic manifold that allow for many possible configurations. And, as mentioned previously, a constraint can be eliminated if the absorption/emission overlap between two molecules in zero. Appendix C contains a simple analysis of the exciton gate's robustness to deviations from the magic angle, in the model case of two chromophores.

We note that classical error correction [37], an indispensable subfield of computer science, may be useful in mitigating imperfections in excitonic cicuits, especially if one were to create particularly complex circuits.

VI. TRANSIENT AND STEADY-STATE SIMULATIONS

In this section we perform numerical simulations of error-prone exciton gates. First we consider the transient case, in which certain states are assumed to have initial excitations, and the system is propagated without external input. Next we simulate the steady state, in which there is a continuous external light input.

In the transient case, Bayes' theorem can be used to determine the likelihood that a true positive, false positive, true negative, or false positive has occurred. Consider our three-molecule exciton gate system consisting of molecules C, G, and E. We consider the effects of G's decay rate γ, set to the same value for $G2 \rightarrow G1$ and $G1 \rightarrow G0$, as well as k_u, which is the rate of undesired transfer from $G1$ to Ee, arising due to imperfect geometric constraints. These are studied in terms of ratios relative to k, which is the rate of each of the desired energy transfer processes.

In our simple gate example, a positive signal ("+") denotes molecule E fluorescing, and a negative ("−") denotes no signal from molecule E. Assuming an ideal gate, the "correct" result would either be ON ("1") or OFF ("0"). We consider two initial states, both with E in the ground state. Initial state $(Ce, G0)$ ought to produce a negative, or "0" result, while initial state $(Ce, G1)$ ought to produce a positive, or "1." $P(1|+)$ denotes the probability of a true positive, i.e. the probability that the gate would have fluoresced in the ideal case, given that the actual signal was positive. For true positives, for instance, Bayes theorem yields:

$$P(1|+) = \frac{P(+|1)P(1)}{P(+|1)P(1) + P(+|0)P(0)}. \qquad (2)$$

$P(0|+)$, $P(1|-)$, and $P(0|-)$ denote probabilities for a false positive, false negative, and true negative, respectively. We assume a uniform prior such that $P(0) = P(1) = \frac{1}{2}$. $P(+|0)$, $P(+|1)$, $P(-|0)$, and $P(-|1)$ are determined from simulations. Additional numerical details of the rate model are given in Appendix A.

Results for the transient case are shown in Figure 5. A higher decay rate naturally leads to fewer positive signals, which adversely affects the true negative rate. Conversely, the probability of a true positive is relatively robust to decay rate, at the expense of an increased number of false negatives.

The undesired transfer rate k_u has the opposite effect, as true negatives are quite robust to k_u while true positives are not. Intuitively, this is because the undesired transfer increases the number of false positives.

In the steady-state analysis, we simulated a Type A AND operation, with steady light input provided for the two logical inputs. This numerical experiment provides some insight into how robust a logical operation in a true excitonic circuit is, with respect to errors. We studied this operation because it is the most complex of the six

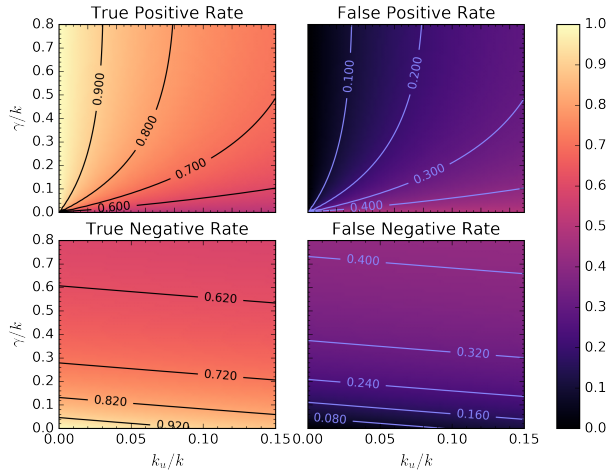

FIG. 5: Results for a transient numerical rate model of the three-molecule construction of an S2 exciton gate. k_u is the rate of undesired transfer processes that were meant to be suppressed by controlled orientations, and γ is the decay rate of the excitations on the gate molecule. Two initial conditions were simulated: $(Ce, G0)$, which for an ideal gate ought produce a negative signal, and $(Ce, G1)$, which ought to produce a positive signal. This is a transient simulation in the sense that there is no input of light after the initial condition is set. Results show that greater k_u increases the false positive rate, and greater γ increases the false negative rate.

binary operations in Figure 3, and hence is likely to be the least robust to errors. Results are shown in Figure 6. Binary inputs x and y are set to "1" by pumping the appropriate molecule with light, while the molecule directly above the first gate molecule ("AND Type A" in Figure 4) is always pumped.

For the parameter ranges shown, different error parameters (γ and k_u) produce different relative probabilities of an exciton reaching the final molecule. n the simulations, we set $k_{migr} = k$, where k_{migr} is the rate at which the exciton migrates on to the next molecule in the exciton circuit. For the molecules that are pumped, the excitation rate and decay rate are arbitrarily set to 0.4 and 0.2, respectively. Undesired transfers occur from each G molecule's S1 state to its output molecule's S1 state.

This steady-state numerical result corresponds to the following hypothetical rudimentary application. Consider two macromolecules whose presence in solution we are interested in determining. We are interested only in whether both species are present–hence the AND operation. The two macromolecules have been tagged with appropriate chromophores to complete the AND circuit, and will attach to the exciton circuit via complementary DNA origami strands, to complete the circuit while in the proper orientation. We can observe whether both tagged species are present, by shining continuous light and measuring the intensity of emission. The results show similar trends to those of the transient simulation: higher γ increases false negative rates, while higher k_u increases false positive rates.

The purpose of this steady-state analysis is to determine whether an experiment would be able to be differentiate between a true ON result and a true OFF result, where x and y are inputs to the AND operation. Because the largest errors occur in the case of (x,y)=(0,1), for a worst-case comparison we plot the quotient of (x,y)=(0,1) and (1,1). For the range of parameters shown, the two signals would be distinguishable because they would emit substantially different intensities (a smaller number on the bottom plot of Figure 6 means that the signals are more easily distinguished). The error trends are the same as the true positive case discussed above. These numerical results demonstrate that very substantial decay rates and undesired processes' rates (the latter coming from imprecisions in orientational constraints) can still produce S2 exciton gates that make up useful excitonic circuits.

Note that FRET transfer rates can easily be made to lie within 1 to 10 picoseconds. (Exciton transfer can be substantially faster than 1 ps, but such a high rate would probably arise from the coherent regime, under which the energy levels may change, which makes the design constraints more complex.) Our numerical results show that an S2 exciton gate can function even when γ and k are of similar orders of magnitude. Since typical internal conversion rates are on the order of 0.1 to 10 picoseconds, these numerics suggests that even dyes that we might have naively considered to be poor candidates for G molecules–perhaps a dye with an S2 $\rightarrow$ S1 decay times of 10 ps–may in fact form exciton gates with acceptable fidelities.

VII. CONCLUSION

We have proposed the design of an exciton gate that can be used to control exciton transfer through organic chromophoric systems, and showed theoretically how it may be used to create excitonic binary logic operations. The gate allows energy to flow through its S2 excited state but not its S1 excited state. The two main challenges to overcome in an experimental implementation are short-lived S2 states and the generation of false positives because of poor control over molecular orientations. With careful choice of gate molecules as well as precise placement of the relative orientations of the species, an experimental demonstration is possible. This design may lead to applications in microscopy, photocatalysis, and chemical sensing.

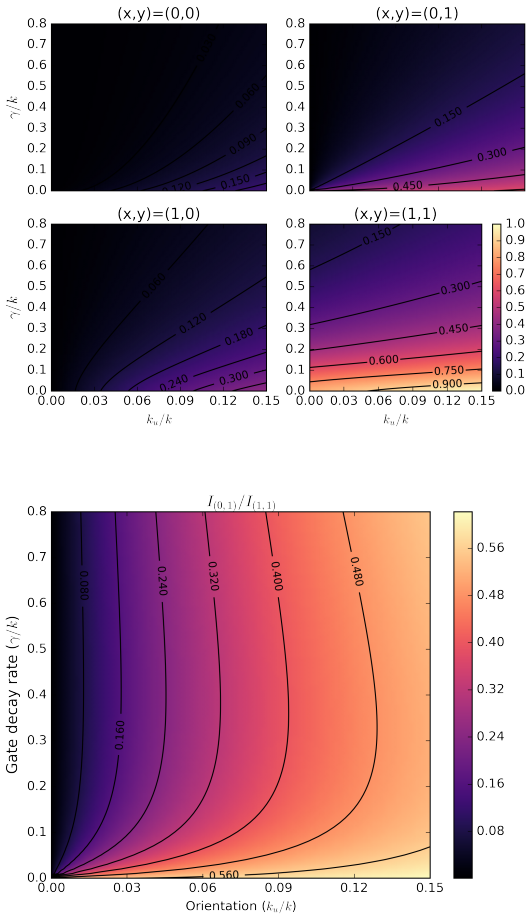

FIG. 6: Even highly imperfect exciton gates can be useful, as long as the difference in intensity between ON and OFF outputs can be easily distinguished. Here we perform a steady state simulation of an imperfect AND gate (Type A). γ is the decay rate on the gate molecules, and k_u is the rate of undesired transfer from a G1 state to an E1 state. Top: Logical AND gate for the four unique two-bit inputs, where the steady-state population on the output chromophore is plotted. This can be interpreted as the fluorescence intensity from an output molecule. Bottom: The quotient of transferred population, between (x,y) inputs (0,1) and (1,1), is plotted. For most values shown, the difference in intensity would make it easy to distinguish between true positives and false positives.

ACKNOWLEDGEMENTS

This work was funded by the Center for Excitonics, an Energy Frontier Research Center funded by the U.S. Department of Energy, Office of Science and Office of Basic Energy Sciences, under Award Number DE-SC0001088. This work was also supported by the STC Center for Integrated Quantum Materials, NSF Grant No. DMR-1231319. A. A.-G. is very thankful to the Canadian Institute for Advanced Research (CIFAR) for their generous support and collaborations. We are grateful for useful conversations with Thomas Markovich, Semion Saikin, Doran Bennett, Marc Baldo, and Roland Lindh.

Appendix A: Numerical details

We use a simple rate model to study the effect of decay and transfer rates. The model includes just three processes: exciton decay, light-induced pumping to the excited state, and exciton transfer. Transfer is assumed to take place via incoherent Förster hopping, though in the future it would be possible to extend the model to the quantum regime, using an open quantum systems formalism such as the Lindblad equation [38].

In defining the state space, naively one may expect the following to be sufficient:

$$x = \begin{bmatrix} Cg \\ Ce \\ 0 \\ 1 \\ 2 \\ Eg \\ Ee \end{bmatrix} \tag{A1}$$

However, it is clear that such a state space would not allow for conditional probabilities. For example, there would not be two separate matrix elements that distinguish between $(Ce, 1) \to (Cg, 2)$ and $(Ce, 0) \to (Cg, 2)$.

Instead, a Hilbert-like space is required in order to properly design operators. For the three-molecule construction, the state space would be defined as

$$x = \begin{bmatrix} Cg \\ Ce \end{bmatrix} \otimes \begin{bmatrix} 0 \\ 1 \\ 2 \end{bmatrix} \otimes \begin{bmatrix} Eg \\ Ee \end{bmatrix} \tag{A2}$$

Appendix B: Heterodimer design

It may be possible to design a gate (G) molecule using two coherently interacting dyes (the dimer itself would behave as one G molecule). This would allow for tunable energy levels and tunable relative orientations between $\hat{\mu}[G_0^1]$ and $\hat{\mu}[G_1^2]$, assuming one has strong control over the orientation and positions of the dimer. A heterodimer is required, since a homodimer would produce parallel transition dipole moments, which would violate the geometric constraints. The following equations [28] describe the excited states of a strongly interacting dimer, where J is the exciton coupling, ϵ denotes an energy, θ is called the mixing angle, and $\vec{\mu}$ denotes the transition dipole vector. Labels a and b denote the monomer, ϕ and χ denote the singly excited delocalized states, ee denotes the doubly excited state.

$$tan2\theta = \frac{2J}{\epsilon_a - \epsilon_b} \tag{B1}$$

$$\begin{aligned} |\phi\rangle &= cos\theta|eg\rangle + sin\theta|ge\rangle \\ |\chi\rangle &= -sin\theta|eg\rangle + cos\theta|ge\rangle \\ |ee\rangle &= |ee\rangle \end{aligned} \tag{B2}$$

$$\begin{aligned} \epsilon_\phi &= \frac{\epsilon_a + \epsilon_b}{2} - \frac{\epsilon_a - \epsilon_b}{2} sec2\theta \\ \epsilon_\chi &= \frac{\epsilon_a + \epsilon_b}{2} + \frac{\epsilon_a - \epsilon_b}{2} sec2\theta \\ \epsilon_{ee} &= \epsilon_a + \epsilon_b \end{aligned} \tag{B3}$$

$$\begin{aligned} \vec{\mu}_\phi &= \vec{\mu}_a cos\theta + \vec{\mu}_b sin\theta \\ \vec{\mu}_\chi &= -\vec{\mu}_a sin\theta + \vec{\mu}_b cos\theta \\ \vec{\mu}_{\phi-ee} &= \vec{\mu}_a sin\theta + \vec{\mu}_b cos\theta \\ \vec{\mu}_{\chi-ee} &= \vec{\mu}_a cos\theta - \vec{\mu}_b sin\theta \end{aligned} \tag{B4}$$

Decoherence and relaxation [16, 38] would need to be considered while designing such a dimer. Also note that it would be most useful to choose monomers that have dark S2 states, as this would help prevent exciton transfer from the $|ee\rangle$ (doubly excited) state to an S2 monomer state.

This design of course produces three excited states ($|\phi\rangle$, $|\chi\rangle$, and $|ee\rangle$), whereas our ideal gate molecule G ought to have two excited states. This can be dealt with in one of two ways. First, the molecules may be spatially arranged such that the first transition is dark: $\vec{\mu}_\phi = 0$ (i.e., $\vec{\mu}_a cos\theta = -\vec{\mu}_b sin\theta$). Hence just one intermediate state ($|\chi\rangle$) would be accessible from the ground state, from which the $|ee\rangle$ state is accessible. Gate imperfections may arise if the intermediate state decays to the dark state $|\phi\rangle$ and gets stuck there. The second option is to ensure that the energy gap in molecule C is smaller than ϵ_ϕ (preventing FRET to $|\phi\rangle$) but greater than the gap between $|\chi\rangle$ and $|ee\rangle$.

Appendix C: Relationship Between Transfer Rates and Orientation Factor κ

In the dipole-dipole approximation, the FRET transfer rate between two molecular electronic states (labelled process j) is proportional to the square of κ divided by the inter-chromophore distance (R) to the sixth power,

$$k_j \propto \frac{\kappa_j^2}{R_j^6}. \tag{C1}$$

To obtain a rough general estimate for how much κ may be allowed to deviate from zero, we compare the rate of desired transfer, k, to the rate of undesired transfer, k_u. We assume that R is the same for both rates. Additionally, Figure 6 suggests that k_u/k may be as high as 0.15 for an AND Type A operation, while still allowing for a clear distinction between the steady-state signal of a binary-on and binary-off.

Here we arbitrarily choose to calculate limits for κ_u (the orientation factor associated with the undesired transfer process) for κ^2 values of 1 and 4, where κ is the desired transfer's orientation factor. Note that $\kappa^2 > 1$ for nearly half of the domain of θ (defined below), making this a useful pair of values for determining the conditions under which $k_u/k \leq 0.15$.

Inserting $k_u/k \leq 0.15$ into Equation C1 yields a limit for the undesired transfer's κ_u of ± 0.39 and ± 0.77, assuming the desired transfer's κ^2 values of 1 and 4, respectively. These are surprisingly permissive bounds, suggesting that it will not require particularly precise nanoscopic methods to synthesize structures with a sufficiently small κ_u.

It is instructive to further investigate κ_u's dependence on explicit geometric changes. To simplify the analysis, we assume that for each energy transfer process, the two transition dipoles sit on the x-axis, and both dipoles have the same angle θ relative to the x-axis. This allows us to obtain an estimate by modifying just one degree of freedom. Under these constraints, for arbitrary process j,

$$\kappa_j = 1 - 3cos(\theta_j)^2. \tag{C2}$$

For κ_u values of -.77, -.39, +.39, and +.77, Equation C2 yields θ_u (angle for the two transition dipoles that define the undesired transfer) values of 39.8°, 47.1°, 63.2°, 73.9°, respectively. (Note that the magic angle, at which κ=0, is 54.7°.) This provides a window of either 16° or 34°, when considering just the first quadrant of the unit circle. Since Equation C2 crosses the origin four times for $0 \leq \theta \leq 360$, this window of of allowable θ_u appears four times over the unit circle.

In conclusion, this appendix has demonstrated that the transition dipoles' orientational requirements are certainly within reach. Still, the deeper the excitonic circuit is the more precision will be required, as errors propagate.

Appendix D: Screening procedure and results

An initial virtual screening of gate molecules was performed to assess the promise of finding viable candidates. Because azulene and its derivatives are already known to have long-lived second excited states, this initial effort was focused on molecules chemically similar to azulene. The screening library consisted of 180 molecules from two sources: (1) purchasable molecules in the eMolecules database (www.emolecules.com) with the fused five- and seven-ring structure to azulene (including heteroatoms in the fused-ring structure itself), and (2) azulene molecules functionalized by alkyl groups and small rings that had

been used to tune the electronic structure of organic light-emitting diode molecules [18].

Each molecule was subject to a protocol of TD-DFT electronic structure calculations (B3LYP/6-31G(d)) scored on six criteria (from a scale of 0 to 1, with 1 being the most desired) for this initial screening:

1. The S0 to S1 vertical excitation energy (from the S0 minimum) was given a score of 1 if the transition is predicted to be in the visible region (1.6 to 3.3 eV) and given a score of 0 otherwise.

2. Likewise, the S1 to S2 vertical excitation energy (from the S1 minimum) was also scored in the same discrete fashion as the S0 to S1 transition.

3. A rough estimate of the angle between the S0 to S1 and S1 to S2 transitions dipole vectors was obtained at the S0 geometry. The angle between the two vectors then used as the input to the formula

   $||sin(2\phi)||$

   where ϕ is the angle between the two vectors. This function goes to zero when the vectors are coincident. Although this scoring function peaks at 90°, which is not necessarily the optimal angle for these two transitions, these scoring functions mainly serve to exclude molecules rather than provide a definitive ranking at this stage.

4. The oscillator strength of the S0 to S1 vertical transition was scored relative to the population of molecules screened. Here, the median oscillator strength was assigned a score of 0.5. Then, each molecule was evaluated relative to this median molecule according to the formula

   $\frac{1}{3}(log_{10}(\mu)) - log_{10}(\mu_{ref})) + 0.5$

   where μ is the oscillator strength of the molecule of interest and μ_{ref} is the median transition. This score is also capped to be no larger than 1 and no smaller than 0, allowing molecules to have up to 1.5 orders of magnitude less than the median oscillator strength before being considered dark.

5. The oscillator strength of the S1 to S2 vertical transition (this time again from the S0 geometry at this rough screening stage) was evaluated in the same manner as criterion (4), this time with the median S1 to S2 oscillator strength serving as the 0.5-scored reference point.

6. Finally, molecules thought to be prone to intersystem crossing were eliminated. Energy levels of the adiabatic S1, vertical S1, and vertical S2 levels were compared with those of the vertical T1, T2, and T3 levels as a proxy to look for closely spaced potential energy surfaces. Any molecules with energy levels within 0.025 eV (the product of the Boltzmann constant and 300 K) of each other were assigned a score of zero, and minimum gaps outside of this value were scored according to the formula

   $10 \times ||(E_{min} - 0.025)||$

   As with the other scoring functions, this was capped at 1.

Out of the library of 180 molecules, there are 40 molecules that have a non-zero geometric mean of these six scores, indicating that at this initial survey there is a space of promising molecules to be further explored. A more complete multi-step screening procedure, which may search other molecular classes as well as strongly interacting dimers, will be completed in a subsequent study.

The final essential screening criterion is to estimate excited state lifetimes of the G molecules, which would be done in part by finding nearby conical intersections between potential energy surfaces. Though finding conical intersections is computationally much more time-consuming than calculating the molecules' other relevant properties, such calculations are possible to perform [29–31].

[1] Y. Benenson, B. Gil, U. Ben-Dor, R. Adar, and E. Shapiro, "An autonomous molecular computer for logical control of gene expression," *Nature*, vol. 429, pp. 423–429, May 2004.

[2] J. Jahns and S. H. Lee, *Optical Computing Hardware: Optical Computing*. Academic press, 1994.

[3] M. L. Perrin, E. Burzuri, and H. S. J. van der Zant, "Single-molecule transistors," *Chem. Soc. Rev.*, vol. 44, pp. 902–919, 2015.

[4] Y. Y. Kuznetsova, M. Remeika, A. A. High, A. T. Hammack, L. V. Butov, M. Hanson, and A. C. Gossard, "All-optical excitonic transistor," *Opt. Lett.*, vol. 35, pp. 1587–1589, May 2010.

[5] P. Andreakou, S. V. Poltavtsev, J. R. Leonard, E. V. Calman, M. Remeika, Y. Y. Kuznetsova, L. V. Butov, J. Wilkes, M. Hanson, and A. C. Gossard, "Optically controlled excitonic transistor," *Applied Physics Letters*, vol. 104, no. 9, p. 091101, 2014.

[6] G. T. Craven and A. Nitzan, "Electrothermal transistor effect and cyclic electronic currents in multithermal charge transfer networks," *Phys. Rev. Lett.*, vol. 118, p. 207201, May 2017.

[7] B. L. Ferninga and W. R. Browne, *Molecular Switches*. Wiley-VCH, 2011.

[8] Y. Yan, M. E. Marriott, C. Petchprayoon, and G. Marriott, "Optical switch probes and optical lock-in detection (olid) imaging microscopy: high-contrast fluorescence imaging within living systems," *Biochemical Journal*, vol. 433, no. 3, pp. 411–422, 2011.

[9] W. Szymaski, J. M. Beierle, H. A. V. Kistemaker, W. A.

Velema, and B. L. Feringa, "Reversible photocontrol of biological systems by the incorporation of molecular photoswitches," *Chemical Reviews*, vol. 113, no. 8, pp. 6114–6178, 2013.

[10] S. Karthikeyan and R. P. Sijbesma, "Probing strain in thermoplastic elastomers using fluorescence resonance energy transfer," *Macromolecules*, vol. 42, no. 14, pp. 5175–5178, 2009.

[11] S. W. Hong and W. H. Jo, "A fluorescence resonance energy transfer probe for sensing ph in aqueous solution," *Polymer*, vol. 49, no. 19, pp. 4180 – 4187, 2008.

[12] J. Waluk, *Conformational analysis of molecules in excited states*, vol. 22. John Wiley & Sons, 2000.

[13] L. Wei, Z. Chen, L. Shi, R. Long, A. V. Anzalone, L. Zhang, F. Hu, R. Yuste, V. W. Cornish, and W. Min, "Super-multiplex vibrational imaging," *Nature*, vol. 544, no. 7651, pp. 465–470, 2017.

[14] N. J. Turro, *Modern molecular photochemistry*. University science books, 1991.

[15] M. Kasha, "Characterization of electronic transitions in complex molecules," *Discuss. Faraday Soc.*, vol. 9, pp. 14–19, 1950.

[16] V. May and O. Khn, *Charge and energy transfer dynamics in molecular systems*. John Wiley & Sons, 2008.

[17] R. S. Bohacek, C. McMartin, and W. C. Guida, "The art and practice of structure-based drug design: A molecular modeling perspective," *Medicinal Research Reviews*, vol. 16, no. 1, pp. 3–50, 1996.

[18] R. Gomez-Bombarelli, J. Aguilera-Iparraguirre, T. D. Hirzel, D. Duvenaud, D. Maclaurin, M. A. Blood-Forsythe, H. S. Chae, M. Einzinger, D.-G. Ha, T. Wu, G. Markopoulos, S. Jeon, H. Kang, H. Miyazaki, M. Numata, S. Kim, W. Huang, S. I. Hong, M. Baldo, R. P. Adams, and A. Aspuru-Guzik, "Design of efficient molecular organic light-emitting diodes by a high-throughput virtual screening and experimental approach," *Nat Mater*, vol. 15, pp. 1120–1127, Oct 2016. Article.

[19] M. Beer and H. C. LonguetHiggins, "Anomalous light emission of azulene," *The Journal of Chemical Physics*, vol. 23, no. 8, pp. 1390–1391, 1955.

[20] S. Murata, C. Iwanaga, T. Toda, and H. Kokubun, "Fluorescence yields of azulene derivatives," *Chemical Physics Letters*, vol. 13, no. 2, pp. 101 – 104, 1972.

[21] S. Schmitt, M. Baumgarten, J. Simon, and K. Hafner, "2,4,6,8-tetracyanoazulene: A new building block for organic metals," *Angewandte Chemie International Edition*, vol. 37, no. 8, pp. 1077–1081, 1998.

[22] N. Tetreault, R. S. Muthyala, R. S. H. Liu, and R. P. Steer, "Control of the photophysical properties of polyatomic molecules by substitution and solvation: The second excited singlet state of azulene," *The Journal of Physical Chemistry A*, vol. 103, no. 15, pp. 2524–2531, 1999.

[23] R. S. H. Liu, R. S. Muthyala, X.-s. Wang, A. E. Asato, P. Wang, and C. Ye, "Correlation of substituent effects and energy levels of the two lowest excited states of the azulenic chromophore," *Organic Letters*, vol. 2, no. 3, pp. 269–271, 2000. PMID: 10814299.

[24] P. Foggi, F. V. R. Neuwahl, L. Moroni, and P. R. Salvi, "S1 sn and s2 sn absorption of azulene: Femtosecond transient spectra and excited state calculations," *The Journal of Physical Chemistry A*, vol. 107, no. 11, pp. 1689–1696, 2003.

[25] H. Ghosh, "A possible route to the violation of vavilovkasha rule in π-conjugated polymers," *Chemical Physics Letters*, vol. 426, no. 4, pp. 431 – 435, 2006.

[26] S. V. Frolov, Z. Bao, M. Wohlgenannt, and Z. V. Vardeny, "Ultrafast spectroscopy of even-parity states in π-conjugated polymers," *Phys. Rev. Lett.*, vol. 85, pp. 2196–2199, Sep 2000.

[27] S. V. Frolov, Z. Bao, M. Wohlgenannt, and Z. V. Vardeny, "Excited-state relaxation in π-conjugated polymers," *Phys. Rev. B*, vol. 65, p. 205209, May 2002.

[28] T. Manal and G. R. Fleming, "Probing electronic coupling in excitonically coupled heterodimer complexes by two-color three-pulse photon echoes," *The Journal of Chemical Physics*, vol. 121, no. 21, pp. 10556–10565, 2004.

[29] Y. Shao, Z. Gan, E. Epifanovsky, A. T. Gilbert, M. Wormit, J. Kussmann, A. W. Lange, A. Behn, J. Deng, X. Feng, D. Ghosh, M. Goldey, P. R. Horn, L. D. Jacobson, I. Kaliman, R. Z. Khaliullin, T. Ku, A. Landau, J. Liu, E. I. Proynov, Y. M. Rhee, R. M. Richard, M. A. Rohrdanz, R. P. Steele, E. J. Sundstrom, H. L. W. III, P. M. Zimmerman, D. Zuev, B. Albrecht, E. Alguire, B. Austin, G. J. O. Beran, Y. A. Bernard, E. Berquist, K. Brandhorst, K. B. Bravaya, S. T. Brown, D. Casanova, C.-M. Chang, Y. Chen, S. H. Chien, K. D. Closser, D. L. Crittenden, M. Diedenhofen, R. A. D. Jr., H. Do, A. D. Dutoi, R. G. Edgar, S. Fatehi, L. Fusti-Molnar, A. Ghysels, A. Golubeva-Zadorozhnaya, J. Gomes, M. W. Hanson-Heine, P. H. Harbach, A. W. Hauser, E. G. Hohenstein, Z. C. Holden, T.-C. Jagau, H. Ji, B. Kaduk, K. Khistyaev, J. Kim, J. Kim, R. A. King, P. Klunzinger, D. Kosenkov, T. Kowalczyk, C. M. Krauter, K. U. Lao, A. D. Laurent, K. V. Lawler, S. V. Levchenko, C. Y. Lin, F. Liu, E. Livshits, R. C. Lochan, A. Luenser, P. Manohar, S. F. Manzer, S.-P. Mao, N. Mardirossian, A. V. Marenich, S. A. Maurer, N. J. Mayhall, E. Neuscamman, C. M. Oana, R. Olivares-Amaya, D. P. ONeill, J. A. Parkhill, T. M. Perrine, R. Peverati, A. Prociuk, D. R. Rehn, E. Rosta, N. J. Russ, S. M. Sharada, S. Sharma, D. W. Small, A. Sodt, T. Stein, D. Stck, Y.-C. Su, A. J. Thom, T. Tsuchimochi, V. Vanovschi, L. Vogt, O. Vydrov, T. Wang, M. A. Watson, J. Wenzel, A. White, C. F. Williams, J. Yang, S. Yeganeh, S. R. Yost, Z.-Q. You, I. Y. Zhang, X. Zhang, Y. Zhao, B. R. Brooks, G. K. Chan, D. M. Chipman, C. J. Cramer, W. A. G. III, M. S. Gordon, W. J. Hehre, A. Klamt, H. F. S. III, M. W. Schmidt, C. D. Sherrill, D. G. Truhlar, A. Warshel, X. Xu, A. Aspuru-Guzik, R. Baer, A. T. Bell, N. A. Besley, J.-D. Chai, A. Dreuw, B. D. Dunietz, T. R. Furlani, S. R. Gwaltney, C.-P. Hsu, Y. Jung, J. Kong, D. S. Lambrecht, W. Liang, C. Ochsenfeld, V. A. Rassolov, L. V. Slipchenko, J. E. Subotnik, T. V. Voorhis, J. M. Herbert, A. I. Krylov, P. M. Gill, and M. Head-Gordon, "Advances in molecular quantum chemistry contained in the Q-Chem 4 program package," *Molecular Physics*, vol. 113, no. 2, pp. 184–215, 2015.

[30] L. Serrano-Andrs and M. Merchn, "Quantum chemistry of the excited state: 2005 overview," *Journal of Molecular Structure: THEOCHEM*, vol. 729, no. 1, pp. 99 – 108, 2005. Proceedings of the 30th International Congress of Theoretical Chemists of Latin Expression.

[31] J. M. Herbert, X. Zhang, A. F. Morrison, and J. Liu, "Beyond time-dependent density functional theory using only single excitations: Methods for computational stud-

ies of excited states in complex systems," *Accounts of Chemical Research*, vol. 49, no. 5, pp. 931–941, 2016.

[32] S. Mukamel, *Principles of nonlinear optical spectroscopy*. Oxford University Press, 1999.

[33] T. Torring, N. V. Voigt, J. Nangreave, H. Yan, and K. V. Gothelf, "Dna origami: a quantum leap for self-assembly of complex structures," *Chem. Soc. Rev.*, vol. 40, pp. 5636–5646, 2011.

[34] E. Schwartz, S. Le Gac, J. J. L. M. Cornelissen, R. J. M. Nolte, and A. E. Rowan, "Macromolecular multi-chromophoric scaffolding," *Chem. Soc. Rev.*, vol. 39, pp. 1576–1599, 2010.

[35] M. C. So, G. P. Wiederrecht, J. E. Mondloch, J. T. Hupp, and O. K. Farha, "Metal-organic framework materials for light-harvesting and energy transfer," *Chem. Commun.*, vol. 51, pp. 3501–3510, 2015.

[36] B. Albinsson and J. Mrtensson, "Long-range electron and excitation energy transfer in donorbridgeacceptor systems," *Journal of Photochemistry and Photobiology C: Photochemistry Reviews*, vol. 9, no. 3, pp. 138 – 155, 2008.

[37] M. Tomlinson, C. J. Tjhai, M. A. Ambroze, M. Ahmed, and M. Jibril, *Error-Correction Coding and Decoding*. Springer, 2017.

[38] H.-P. Breuer and F. Petruccione, *The theory of open quantum systems*. Oxford University Press, 2002.